Available online at www.sciencedirect.com
SCIENCE DIRECT®
Journal of Photochemistry and Photobiology A: Chemistry 169 (2005) 235–251
Journal of Photochemistry and Photobiology A:Chemistry
www.elsevier.com/locate/jphotochem

Photocatalyzed oxidation and mineralization of C1–C5 linear aliphatic acids in UV-irradiated aqueous titania dispersions—kinetics, identification of intermediates and quantum yields☆

Nick Serpone[a,*,1], Jean Martin[b], Satoshi Horikoshi[c], Hisao Hidaka[c]

[a] *Dipartimento di Chimica Organica, Università di Pavia, 10 via Taramelli, 27100 Pavia, Italy*
[b] *Pharmetics Inc., 3695 Autoroute des Laurentides, Laval, Que., Canada H7L 3H7*
[c] *EPFC Center and Department of Chemistry, Meisei University, 2-1-1 Hodokubo, Hino-shi, Tokyo, Japan*

Received 24 May 2004; received in revised form 28 June 2004; accepted 2 July 2004
Available online 14 August 2004

Abstract

The photocatalyzed degradation and mineralization of the linear carboxylic acid C1–C5 series (namely, formic acid, acetic acid, propanoic acid, butanoic acid, and valeric acid) were examined in UV-irradiated air-equilibrated aqueous TiO_2 dispersions: (a) to assess the extent of (dark) adsorption and photoadsorption; (b) to determine their relationship with degradation; (c) to elucidate the dynamics of the degradative and mineralization processes (as loss of total organic carbon); (d) to identify intermediates by liquid chromatography (HPLC), gas chromatography (GC–FID) and gas chromatography coupled to a mass detector (GC–MS), and (e) to determine the quantum yields of degradation of this linear acid series based on formic acid ($\Phi = 0.12 \pm 0.02$) as a secondary actinometer proposed for aliphatic substrates. At low catalyst loading (2.0 g/L) and except for formic acid, adsorption of the other four C2–C5 acids increased with chain length, although the overall level was rather small, contrary to high catalyst loading (20 g/L) where all four C2–C5 acids adsorbed to nearly the same extent (15–19%) with adsorption of formic acid on TiO_2 being two-fold greater (34%). The dynamics of degradation and mineralization decreased with increase in chain length, i.e. formic acid degraded and mineralized faster than its longer chain congeners. Several intermediates were identified in the degradation of the C3–C5 acids; in particular, 21 species were positively identified in the degradation of valeric acid by the techniques used. On the basis of partial charges and frontier electron densities of all atoms of the carboxylic acids, together with known species formed a route is proposed for valeric acid degradation. The quantum yields of degradation for the C2–C5 acid series increased with chain length from $\Phi = 0.010$ for acetic acid to $\Phi = 0.067$ for valeric acid.

Keywords: Photodegradation; Photomineralization; Saturated linear C1–C5 carboxylic acids; Quantum yields of photodegradation; Intermediates

1. Introduction

Aliphatic carboxylic acids perform a diverse range of industrial functions. Some occur naturally serving an important function in nutrition (e.g. acetic acid), whereas many others are intermediates in normal biochemical processes [1]. The level of industrial production of some of these acids demonstrates their commercial and industrial relevance. For example, the annual production of acetic acid revolves around 1.5×10^6 metric tons, acrylic acid around 0.5 million metric tons, and propionic acid about 45,000 metric tons. Some short chain aliphatic acids can cause acute adverse effects to skin, eyes, and mucuous membranes [1]. In the metabolism of aliphatic acids, cytochrome P450 can interact with such acids to produce a metabolite toxic to the liver. Some aliphatic

☆ Taken in part from the part-time M.Sc. Thesis of Jean Martin (1996–2003), Concordia University, Montreal, Canada.

* Corresponding author. Tel.: +39 0382 507835; fax: +39 0382 507323.
E-mail addresses: nick.serpone@unipv.it, serpone@vax2.concordia.ca, serpone@videotron.ca (N. Serpone).
[1] Professor Emeritus, Concordia University, Montreal, Canada.

1010-6030/$ – see front matter © 2004 Elsevier B.V. All rights reserved.
doi:10.1016/j.jphotochem.2004.07.001

acids have also been shown to have a teratogenic effect on laboratory animals [2], while aliphatic aldehydes and dicarboxylic acids have been shown to be carcinogens to some female rodents [3]. The anti-convulsant 2-propylpentanoic acid is teratogenic in humans and rodents [4]. Another C8 aliphatic acid, octanoic acid, is known to be toxic to several insect species [5].

If the TiO_2 photocatalytic process, one of several advanced oxidation processes (AOP) examined for environmental remediation, is to find a niche in water purification treatments at the industrial scale to produce drinking water that meets quality standards, determination of the extent to which a specific contaminant can be degraded is clearly of primary importance. In this regard, TiO_2-mediated photocatalytic studies in aqueous media of aliphatic acids with more than two C atoms have been rather scarce [6–11], and at times were performed in oxygen-free aqueous media [8,9] to yield aldehydes (and/or ketones) and alkanes as intermediary species [13] and 4-oxopentanoic acid [9] for the C2–C4 acids. Heptanol and heptanoic acid were identified in the TiO_2 photocatalyzed degradation of octanoic acid [10]. The latter study proposed that degradation occurs through the intervention of either the valence band holes (h^+) or $^\bullet$OH radicals to produce alkyl radicals $R^\bullet$, which subsequently react with molecular oxygen O_2 to give alkylperoxy radicals. The latter path was also suggested in the photocatalytic degradation of dodecane (and derivatives) to yield monocarboxylic acids in low yields [12]. Decarboxylation was proposed as the principal route to mineralization of the aliphatic acids in many of these studies.

Germane to the present study, Guillard [6] recently reported the degradation of butanoic acid in aqueous TiO_2 dispersions and in O_3/UV aqueous acidic media (pH 3.6) at which the acid is in its molecular form and in neutral media (pH 6.9) in which the acid is in its dissociated form. In acidic media, the major intermediates were acetic acid (AA), 3-oxobutanoic acid (3-KBA), and propanoic acid (PA) with additional trace quantities of acidic species. In neutral media the intermediates were AA, 3-KBA, PA, 2-butenoic acid, formic acid (FA), oxalic acid, and 2-KBA; some quantities of ethane and propane were also quantified. Comparison of the intermediates produced from the TiO_2 photocatalytic process with those from the degradation of butanoic acid in aqueous O_3/UV media at pH 3.6 deduced [6] the participation of h^+ in the formation of propanoic acid, alkanes and alkenes distinguishing h^+ from surface-bound $^\bullet$OH radicals. However, closer analysis and our earlier pulse radiolytic studies on the chemical entity denoted as h^+ [13] show that h^+ is but the surface-bound $O^{\bullet-}$ species in deprotonated form and surface-bound $^\bullet$OH radicals in acidic media. Accordingly, the distinction between h^+ and $^\bullet$OH is a moot point. Moreover, our more recent studies [14] have shown that pH-dependent surface potentials affect the selectivity of the TiO_2 photocatalyst and that selectivity is also wavelength-of-irradiation dependent, so that differences in the nature of the intermediates produced [6] may have a different origin and unlikely to be the result of h^+ versus $^\bullet$OH radical involvement. Others have reported the photodegradation of dicarboxylic acids in homogeneous phase involving iron(III) salts [15].

Linear C1–C5 carboxylic acids were examined in this study. The corresponding branched isomers (e.g.: 2-methylpropanoic acid) will be reported elsewhere [16]. The acids were exposed to UV radiation in aqueous TiO_2 suspensions to determine the extent to which they are degraded by the TiO_2 photocatalytic method. Rates of degradation of these acids are compared and intermediate species identified to understand how they degrade to CO_2 and water. Several intermediates were identified by liquid chromatography (HPLC), HPLC co-elution methods, gas chromatography (flame ionization detection; GC–FID) and by gas chromatography coupled to mass detection (GC–MS). Process dynamics were resolved for both degradation of substrates and loss of total organic carbon (TOC). Rates of degradation should correlate with C–H bond energies when involving $^\bullet$OH radical participation in oxidative processes [17]. The quantum yield of formic acid was determined and is propsoed as a secondary chemical actinometer for the degradation of aliphatics in the same manner that phenol was proposed for aromatics [18].

2. Experimental section

2.1. Chemicals

Chemicals were obtained from Aldrich and used as received: formic acid, glacial acetic acid, propanoic acid, butanoic acid (BA), valeric acid (VA), and acrylic acid. TiO_2 was Degussa P25; its properties are now well established. GC test solution {split capillary inlet sample; C_{16}/C_9 ratio 1.016; 1% (w/w) *n*-nonane (C_9) and *n*-hexadecane (C_{16}) in *n*-tetradecane (C_{14})} was from Hewlett Packard. Anhydrous $MgSO_4$ and the BSTFA + TMCS (99:1; Sylon BFT) derivatizing agent were obtained from Supelco Canada. Other chemicals were of reagent grade quality.

2.2. Reactors and irradiation

Reactor-1 was a double-walled Pyrex reactor (ca. 60 ml) mounted with an outlet and an inlet port allowing water circulation and temperature control (20 ± 1 °C). Reactor-2 was a single-walled circular Pyrex reactor (ca. 500 mL) with two diametrically opposite flat windows. Irradiation was achieved using an Oriel 1000 W Hg/Xe arc lamp light source. A Pyrex water bath positioned between the reactor and the light source filtered out infrared radiation. Dispersions were air-equilibrated at all times. Air-cooled reactor-2 was used for large-scale experiments; temperature was maintained around 20–24 °C.

Determination of photonic efficiencies and quantum yields used a Bausch & Lomb 0.25 m monochromator to obtain nearly monochromatic 365 nm radiation.

2.3. Analyses

Liquid chromatographic (HPLC) analyses were carried out using a Waters 501 isocratic pump mounted with a 20 μL injection loop, a Waters 441 UV absorbance detector (wavelength, 214 nm), a Hewlett-Packard HP3396A integrator, and a Supelco Spherisorb reverse phase C-8 (5 μm, 250 mm × 4.6 mm) HPLC column. Total organic carbon analyses were performed on a Shimadzu TOC-500 analyzer. Gas chromatographic analyses were done on a GC–FID Hewlett-Packard 5890 series II system; GC–MS analyses were carried out on a mass detector coupled to the HP 5890 series II system.

2.4. Procedures

In a typical experiment, a carboxylic acid solution was prepared at a concentration of 9.79×10^{-3} M (ca. 600 mg/L carbon for a C5 acid; 500 mL). Each aliquot was filtered through 0.22 μm filters (MSI #NO1SP01300 or Spartman-3 Teflon membrane) and analyzed by the HPLC technique. The mobile phase was a mixture of MeOH/H_2O 35/65% (v/v); other ratios were used as required. The pH was adjusted to 3.0 with *o*-phosphoric acid; column was kept at ambient temperature.

2.4.1. Dark adsorption measurements (low catalyst load)

A 50.0 mL solution of the C1–C5 acids (2.0×10^{-3} M) was added to a vial containing 2.0 g/L of TiO_2. The dispersion was sonicated for 5 min and stirred in the dark for ca. 90 min. An appropriate aliquot was collected, filtered and then analyzed by HPLC methods; mobile phases were H_2O/MeOH (99/1% (v/v)) for the C1–C3 acids and a solution of H_2O/MeOH (65/35% (v/v)) for the C4 and C5 acids; pH was 3.0 (*o*-phosphoric acid); temperature was ambient.

2.4.2. Dark adsorption measurements (high catalyst load)

A dispersion of 25.0 mL of a 2.0×10^{-3} M valeric acid solution (pH 3.7 adjusted with $HClO_4$ or NaOH) and 20 g/L of TiO_2 was sonicated for 10 min, and then stirred in the dark for another 60 min. The suspension was sampled at the beginning of the stirring period and then every 20 min thereafter. Samples were filtered and analyzed isocratically by HPLC; mobile phase, 35/65% (v/v) MeOH/H_2O solution at pH 3.0 with *o*-phosphoric acid; column was kept at ambient conditions. All manipulations were performed under dark room conditions (dim red light).

The other four C1–C4 acids were treated in a similar manner collecting one sample after the 60 min dark period. The HPLC mobile phase for butanoic acid was the same as for valeric acid, whereas for the C1–C3 acids, it was a solution of H_2O/MeOH (99/1% (v/v)).

2.4.3. Rates of degradation of the C1–C5 carboxylic acids

Fifty milliliters of a 2.0×10^{-3} M solution of an acid {FA, AA, PA, BA, and VA} was added to reactor-1 containing 2.0 g/L of TiO_2 particles. The dispersion was magnetically stirred in the dark for 90 min prior to irradiation. Wavelengths below 320 nm were excluded from the Pyrex reactor to avoid direct photolysis of the acids. Appropriate 400 μL aliquots were collected from reactor-1 at various times but more frequently in the initial stages, following which they were filtered through 0.22 μm filters and subsequently analyzed by HPLC methods; flow rate, 0.8 mL/min for all measurements; column at ambient temperature; pH, 3.0 with *o*-phosphoric acid. Unless noted otherwise, the mobile phases were: (i) H_2O for the C1–C3 acids; (ii) a solution of H_2O/CH_3CN (90/10% (v/v)) for the C_4 acid; and (iii) H_2O/CH_3CN (80/20% (v/v)) for valeric acid.

2.4.4. Rates of loss of TOC for the C1–C5 carboxylic acids

TOC analyses were performed concurrently with HPLC measurements to determine the rates of disappearance of pollutants and loss of TOC. The Shimadzu TOC-500 analyzer range was set at 10 and the flow rate was 150 mL/min; volume injected, 40 μL; calibration of instrument was performed daily prior to analysis using standard potassium hydrogen phthalate.

2.4.5. Identification of oxidized intermediates by HPLC method

In a typical experiment (constant temperature, 20 °C), 60.0 mL of a solution of 600 mg/L of the acid (PA, BA or VA) and 0.12 g of TiO2 (loading, 2.0 g/L) were added to reactor-1. The suspension was stirred for a few seconds, sonicated for 5 min in a sonicator bath, followed by continued stirring for another 60 min in the dark, and then irradiated at wavelengths greater than 320 nm.

Aliquots (1.0 mL) were collected at various times, filtered, and then analyzed for intermediates by HPLC methods; injected volume, 20 μL; the mobile phase was an aqueous solution of H_3PO_4 (pH 3.0) for propanoic and butanoic acids, and a solution of MeOH/H_2O (25/75% (v/v)) at pH 3.0 for valeric acid.

2.4.6. HPLC co-elution experiments

The degraded acid sample was filtered and subsequently a small volume of an aqueous solution of a suspected intermediate was added to the filtrate and analyzed by the HPLC technique. In essence, the co-elution method consisted of: (1) obtaining a chromatogram of the irradiated solution of a given acid; (2) spiking an aliquot of the irradiated acid solution with a pure sample of a suspected potential intermediate; and (3) determining peak overlap between the spiked sample and the irradiated acid. Peak overlap provided positive identification.

2.4.7. Adsorption equilibrium constant K of the C1–C5 acids

A solution (50.0 mL) of the C1–C5 aliphatic acids of various concentrations (4.90×10^{-4} M, 7.34×10^{-4} M, 9.79×10^{-4} M, 1.47×10^{-3} M, 1.96×10^{-3} M, and 5.87×10^{-3} M) was adjusted to pH 3.7 ($HClO_4$ and/or NaOH) and subsequently added to reactor-1 containing 2.0 g/L of TiO_2 particles. The system was stirred in the dark for 60 min, after which a 500 μL aliquot was collected. The remaining dispersion was irradiated, collecting 500 μL samples at various time intervals. They were filtered and isocratically HPLC-analyzed. The relevant mobile phases were: (1) H_2O/MeOH, 99/1% (v/v) for the C1 and C2 acids; (2) 75/25% (v/v) H_2O/MeOH for propanoic acid; and (3) 60/40% (v/v) H_2O/MeOH for the C4 and C5 acids; the pH was 3.0 (*o*-phosphoric acid).

2.5. GC–FID investigation of valeric acid intermediates

2.5.1. Derivatization of acid and intermediates

In a typical experiment, one drop of a pure acid (ca. 13 mg of valeric acid or 1.27×10^{-4} mol) was transferred to a glass vial to which was added 400 μL of the derivatizing agent BSTFA + 1%TMCS {99:1, equivalent to 1.5×10^{-3} mol; minimum BSTFA to labile proton ratio was 12:1 for valeric acid; TMCS is trimethylchlorosilane}. The sample was heated (see below) for 30 min and vortexed every 5 min subsequent to which 2.0 μL of the sample was injected into the HP-5890 series II system.

The efficiency of the derivatization procedure was validated with a simulated sample. Thus, 60.0 mL of an aqueous solution 600 mg/L in valeric acid or butanoic acid was transferred to a separatory funnel, acidified with five drops of concentrated HCl and extracted with three portions of 120 mL of diethyl ether. The ethereal extract was dried over anhydrous $MgSO_4$, filtered in vacuo {Buckner funnel mounted with a 0.22 μm fritted disk} and then followed by evaporation on a rotary evaporator. Subsequently, 3.0 mL of the derivatizing agent was added to the residue under argon. The flask was stoppered and the mixture heated over a water bath (80 °C) for ca. 30 min with magnetic stirring. GC–FID analyses were performed on: (1) the pure derivatizing agent; (2) the derivatized extract (first two of three portions of the 120 mL of ether); and (3) on the last ethereal extract, which was treated in a similar manner (dried, filtered, evaporated, derivatized, and finally heated).

2.5.2. Relative retention times

The relative retention times of all acids were determined against valeric acid and then compared to those obtained for the peaks of a chromatogram for an irradiated valeric acid solution analyzed under the same conditions to identify (some) unknown intermediates. The latter chromatogram was also compared to that of a blank. Sample preparation was: 400 mL of a 600 mg/L valeric acid solution was transferred into reactor-2 containing 2.0 g/L of TiO_2. The suspension was sonicated for 5 min and then irradiated. Temperature was 20–24 °C during the 8 h degradation period, after which the whole suspension was filtered and 60 mL of the filtrate was taken and subsequently treated as described earlier. A blank was prepared by the same procedure but without valeric acid in the irradiated solution.

2.6. GC–MS identification of the intermediates of Valeric acid degradation

A solution (400 mL; ca. 600 mg/L) of valeric acid was irradiated for a given time period, filtered, and the subsequent filtrate components derivatized. The 400 mL blank solution was treated in identical manner. After derivatization, the derivatized residue and the blank were diluted 10-fold with anhydrous diethyl ether, followed by analysis (0.50 μL for each sample) by GC–MS.

The extra peaks found in the chromatogram of the irradiated sample that did not appear in the chromatogram of the blank were used for identification of intermediates with a mass spectral library. The validity of this methodology for valeric acid was ascertained from retention times and on the basis of molecular weights of the expected intermediates.

2.7. Partial charges and frontier electron density calculations of the C1–C5 linear acids

Partial charges and frontier electron densities of all atoms of the linear aliphatic acid series were calculated using the MOPAC/AM1 wavefunction. The computer simulations were carried out using the CAChe Worksystem version 5.04 (Fujitsu Co. Ltd.) implemented on an Intel Pentium-IV and Windows XP system. A geometrical configuration was determined by pre-optimization calculation in Mechanics using augmented MM3, followed by geometrically optimized calculations in MOPAC using AM1 parameters. Solvation effects in water were simulated using COSMO also available in the CAChe package.

2.8. Limiting photonic efficiency of formic acid and quantum yields

Fifty milliliters of a 3.92×10^{-3} M solution of formic acid was added to a reactor containing various pre-weighed amounts of TiO_2 Degussa P25 (0.30, 0.60, 0.90, 1.20, 1.50, 1.80, and 2.10 g/L); pH of the suspension was adjusted to 3.7 (NaOH or $HClO_4$ solutions). Dispersions were then sonicated for 5 min and stirred for 60 min, after which a 400 μL aliquot was collected (in the dark for $t = 0$). Subsequent 400 μL samples were collected at various time intervals during irradiation of the dispersion at 365 nm (temperature, 20 ± 1 °C); they were filtered through 0.22 μm filters and then analyzed by HPLC isocratic methods {wavelength, 214 nm; column, Supelco Spherisob octyl 5 μm, 250 mm × 4.6 mm; mobile phase, 1/99% (v/v) MeOH/H_2O; pH 3.0 with o-phosphoric acid; flow rate, 0.8 mL/min}. Photonic efficiencies were estimated from the photon flow as determined by chemical

actinometry with Aberchrome 540 (absorbance measured at 494 nm). Quantum yields of photodegradation of AA, PA, BA, 2-methylbutanoic (2-MBA) and VA acids are based on formic acid as the secondary chemical actinometer.

3. Results and discussion

3.1. Relation between pH and dark adsorption

Fig. 1a illustrates the extent of adsorption and pH results obtained for the linear C1–C5 carboxylic acids series. Each histogram represents the mean value of several experiments and the error bars denote one standard deviation. The variance around the mean of the pH data was negligible. The pHs of the TiO_2 suspensions of AA, PA, BA, and VA acids were similar; that of formic acid was lower in line with its lower pK_a (3.75) relative to those of the other C2−C5 acids examined: pK_a = 4.75, 4.87, 4.81, and 4.82, respectively, for acetic acid, propanoic acid, butanoic acid, and valeric acid. Adsorption in the dark was highest for formic acid (ca. 5.2% after 90 min exposure to the catalyst) correlating with the pK_a. Adsorption of formic acid on the reactor walls was negligible. The TiO_2 particle surface is neutral around pH 5.5–6 [19], the point of zero charge (pzc), below which the surface is positively charged and negatively charged above pzc. Accordingly, charged solutes will impact on the reaction dynamics if the solute and the semiconductor surface are of like charge, or of opposite charge. At pH 3.3, 26% of formic acid exists in the anionic form, thus favoring adsorption through electrostatic attraction. For the other C2−C5 acids, the pH was 3.7–3.8, slightly greater than for the formic acid dispersion, hence less adsorption in accord with the degree of ionization being smaller than for formic acid. Note that adsorption of the acids can occur either through the carboxylate anion or molecularly in the undissociated form [20].

Adsorption increases with chain length of the acid (Fig. 1a). However, the extent of adsorption of the five C1–C5 linear acids on TiO_2 is rather limited under the conditions used. At higher catalyst loads (e.g. 20 g/L) and at concentrations of organic acid around 2.0×10^{-3} M (as above), the extent of dark adsorption of the C2−C5 acids are nearly

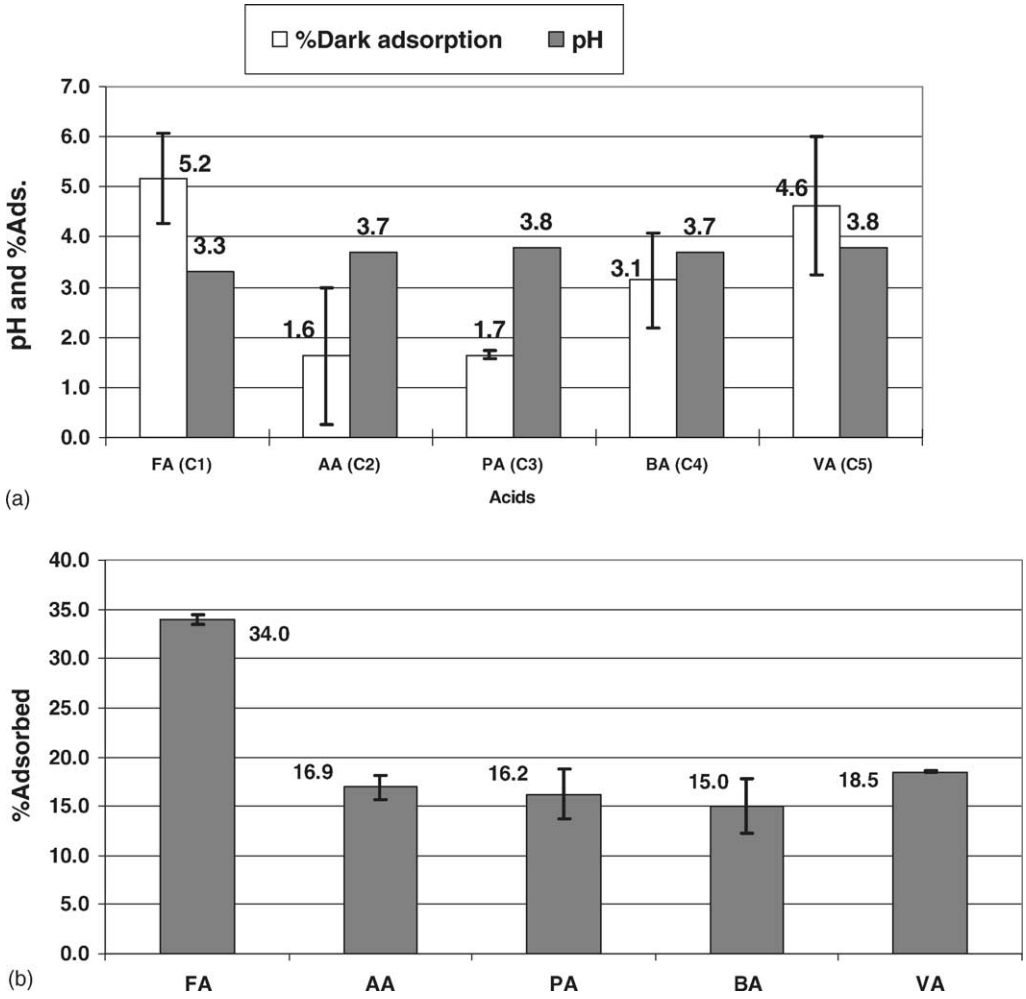

Fig. 1. (a) pH and adsorption of C1–C5 linear carboxylic acids after 90 min in the dark on TiO_2 particles at low catalyst loading of 2.0 g/L. (b) Dark adsorption of selected acids at high TiO_2 loading (20 g/L; pH = 3.7 constant; [acid] = 2.0×10^{-3} M).

identical (ca. 16 ± 1%) in contrast to formic acid with adsorption nearly two-fold greater (ca. 34%; Fig. 1b).

Unlike the data at the lower catalyst loading (Fig. 1a), the suspensions at the 20 g/L catalyst load were maintained at constant pH 3.7 so that the lower the pK_a of an acid the higher was its degree of ionization. Since the pK_a's of the linear C2–C5 acids are relatively similar, the extent of adsorption of these acids on the TiO_2 surface should be nearly the same on electrostatic grounds (Fig. 1b). The major factor impacting the extent of dark adsorption of the linear C1–C5 carboxylic acids is the pH of the medium.

3.2. Adsorption equilibrium constant K in the dark and under UV illumination

The adsorption equilibrium constant in the dark (K_d) was determined by the methodology of Cunningham et al. [21]. Fig. 2a shows the Langmuir-type adsorption isotherm of formic acid, whereas Fig. 2b depicts a plot of the ratio of the concentration of formic acid at equilibrium, $[formic]_{eq}$, to the number of mols of formic acid adsorbed per gram of TiO_2 versus $[formic]_{eq}$. Despite the scatter in the data, saturation was also attained around 2.0×10^{-3} M, in accord with the behavior (R_0 versus C_0) seen in Fig. 3a.

Illumination of TiO_2 particles in dispersions impacts on the adsorption/desorption equilibrium of adsorbed molecules on the surface of TiO_2. Oxygen atoms of metal oxides exchange with oxygen atoms from gaseous molecular O_2 on illumination in the absence of organic species [22]. The TiO_2 particle surface becomes positively charged when UV-irradiated because of formation of H^+ ions from the splitting of water [23]. Moreover, incident photons generate new active sites on the TiO_2 particle leading to changes in the surface characteristics, which also impact on the adsorption/desorption of adsorbates thus making the determination of the number of actives sites a challenging task [18].

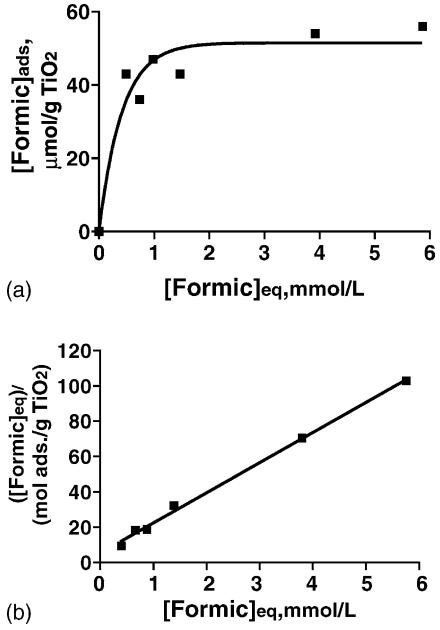

Fig. 2. (a) Langmuir adsorption isotherm plotted as μmols of formic acid adsorbed per gram of TiO_2 in the dark against initial concentration of formic acid. (b) Adsorption isotherm of formic acid on TiO_2 particles plotted as the ratio of the concentration of formic acid at equilibrium $[formic]_{eq}$ to the mols of formic acid adsorbed per gram of TiO_2 against $[formic]_{eq}$.

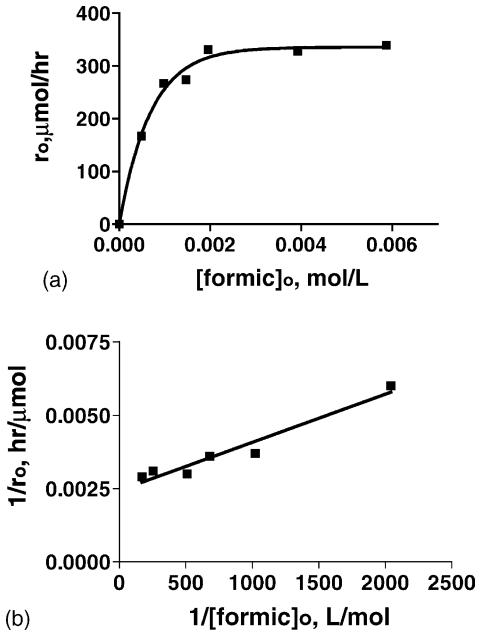

Fig. 3. (a) Langmuir-type plot of initial rates of degradation of formic acid against initial concentration of formic acid. (b) Double reciprocal plot of the rates of degradation of formic acid, $1/r_0$, against initial concentration of formic acid, $1/[formic]_0$.

When surface changes are significant, a noticeable difference can occur in the adsorption/desorption equilibria in the absence and presence of UV illumination. The adsorption/desorption equilibrium constant under illumination was determined kinetically from a plot of $1/R_0$ versus $1/C_0$ (Fig. 3 for formic acid), obtained from a series of degradation experiments carried out at various concentrations but otherwise under identical conditions.

The temporal degradation of formic acid tended to exhibit zero-order kinetics across the concentration range 4.90–58.7 $\times 10^{-4}$ M (see below). The plot of R_0 versus C_0 (Fig. 3a) and the double reciprocal plot $1/R_0$ versus $1/C_0$ (Fig. 3b) show profiles reminiscent of a Langmuir–Hinshelwood adsorption phenomenon with saturation seen at ca. 2.0×10^{-3} M, above which the rates no longer depended on the concentration of formic acid. A similar saturation behavior at ca. 2.0×10^{-3} M was seen for PA and 2-MBA acids.

The adsorption equilibrium constants K_d and K_i (under illumination) for formic acid, propanoic acid, and 2-methylpropanoic acid are reported in Table 1. UV illumination causes K_i for formic acid to be two-fold smaller than K_d in the dark. For propanoic acid, UV illumination of TiO_2 dispersions increases the adsorption equilibrium constant relative to K_d nearly 30-fold, whereas for 2-methylbutanoic acid K_i is four-fold greater than K_d. Hence, photoadsorption of the acids examined is more significant than dark adsorption ex-

Table 1
Adsorption equilibrium constant of selected linear aliphatic acids under UV illumination (K_i) and under dark conditions (K_d)

Acid	K_i ($10^3\,M^{-1}$)	K_d ($10^3\,M^{-1}$)
Formic (FA)	1.51 ± 0.22	3.16 ± 0.10
Propanoic (PA)	5.20 ± 1.11	0.16 ± 0.03
2-Methylbutanoic (2-MBA)	2.57 ± 0.24	0.68 ± 0.26

cept for formic acid, for which photodesorption may be more relevant.

3.3. Complete degradation of C2–C5 acids

Factors that influence the rate of degradation of organic compounds on titanium dioxide include but are not limited to: catalyst load, solute concentration, oxygen concentration, extent of adsorption, pH, photon flow, temperature, presence of inorganic ions, presence of added oxidants, and not least reactor design. Most can be controlled so that observed trends can be rationalized. Herein, catalyst load, solute concentration, photon flow, medium temperature and reactor design were kept constant. No inorganic ions and no oxidants other than O_2 (air) were added as experiments were carried out under air-equilibrated conditions with concentration of oxygen ca. 2.4×10^{-4} M [10]. Rates of reaction may be limited by the rate of electron transfer to oxygen if concentration of solute is greater than 10^{-3} M and the partial pressure of oxygen P_{O_2} is small ($\leq$0.05 atm) [24]. In our study, P_{O_2} was 1 atm and solute concentration was ca. 10^{-3} M. Thus, the only variables were: (i) the pH of the dispersion; and (ii) the extent of adsorption of the organic solute on the catalyst surface. The latter is an intrinsic consequence of the system that may be influenced by the pH of the TiO_2 dispersion. For example, the extent of dark adsorption of organic acids decreases with increasing pH because of repulsion between the anionic form of the acids and the negatively charged TiO_2 surface [21]. The pH of the media was governed by the pK_a of the carboxylic acid.

The temporal degradation of the linear C1−C5 series of carboxylic acids was monitored by HPLC. The absence of a peak of the acid in the chromatograms inferred successful degradation.

The chromatogram for formic acid taken after 30 min of irradiation revealed that degradation of formic acid was complete. The same was observed for the other C2–C5 acids, in that they were completely degraded albeit at longer irradiation times. Hence, the TiO_2 photocatalytic method is an appropriate technique to remove linear organic carboxylic acids from aquatic media. However, the disappearance of a substrate is insufficient for water treatment methods to meet existing governmental standards, since intermediates produced during the degradation process may be more refractory than the parent compounds or else more harmful to human health. For both formic acid and acetic acid, no residual intermediates were detected at the end of the degradative process, at least above the detection limits of the HPLC method. No peak(s) other than the solvent front was observed in the chromatograms, which was not the case for the C3–C5 linear acids. For instance, an intermediate appearing in the chromatograms for propanoic acid was still detectable in solution even though the acid had completely degraded.

This unidentified intermediate from propanoic acid may be: (a) smaller than a C3 organic acid (e.g. AA); (b) an oxidized derivative of propanoic acid {e.g. 2-HPA acid ($CH_3CH(OH)CO_2H$}; (c) a keto derivative of propanoic acid {2-KPA acid, $CH_3C(O)CO_2H$}; or (d) compounds of lower molecular weight or more water soluble than propanoic acid. The intermediate may have less affinity for the reverse phase C-8 column stationary phase. This is not unlikely since lower molecular weight carboxylic acids are typically formed from higher molecular weight compounds [25]. For instance, $^{\bullet}$OH radicals abstract α-H atoms to yield glycolate ($HOCH_2COO^-$) and glyoxylate ($OCHCOO^-$) anions as intermediates in the degradation of acetic acid. Hexanedicarboxylic acid and related dimethyl esters form in the degradation of 1,2-dimethylbenzene [26]. The GC–MS analysis of dodecane intermediates showed the presence of several dodecanone isomers, along with formaldehyde and traces of formic acid [27]. The degradation of 4-ketopentanoic acid produced several intermediates (e.g. 2-oxobutane, propanoic acid, acetic acid, ethanol, acetaldehyde, dimethylketone, ethyl acetate, ethane, methane, and methanol) [9]. In the degradation of butanoic acid, a peak was seen at a higher retention time inferring that the corresponding intermediate had a greater affinity for the column packing, a condition requiring that the species be more hydrophobic than butanoic acid as would occur if the intermediate had a higher carbon load than the parent substrate. Formation of alkyl radicals in such systems can also lead to intermediate products with more carbon atoms than the starting substrates, as demonstrated by the formation of C5 acids (e.g. VA and 2-MBA acids) from propanoic acid [8].

Although the HPLC chromatographic patterns can be rationalized on the basis of existing data, the key issue, however, is that while the C1−C5 acids are completely degraded when exposed to UV irradiation in aqueous TiO_2 dispersions, the total loss of TOC from an irradiated TiO_2 dispersion is a better indicator of photoreaction efficiency as the goal of the photocatalytic process is to mineralize pollutants. In this context, monitoring the disappearance of the organic pollutant can be misleading if it degraded rapidly and the intermediates were refractory to oxidation [28]. Accordingly, we also monitored the amount of TOC left in solution as a function of irradiation time during the degradation of these acids.

The TOC content decreased with time indicating that the C1−C5 acids are mineralized to H_2O and CO_2 albeit not always quantitatively. Except for propanoic acid, where no TOC was detected after 2 h of irradiation, residual amounts (though small) were still present after 2 h of irradiation for formic acid, after 4 h for both acetic acid and butanoic acid, and 4.5 h for valeric acid, although for the C4 and C5 acids the

residuals were statistically negligible. A more detailed TOC analysis is described below where we examine and compare the dynamics of the degradation and the mineralization of the C1−C5 acids.

3.4. Dynamics of degradation and mineralization

The temporal course of the degradation of the C1−C5 linear carboxylic acids (initial concentration, 2.0×10^{-3} M) is illustrated in Fig. 4. Decrease in acid concentration was linear initially and then deviated from linearity at longer irradiation times. For formic acid, the decrease scaled linearly for the first 20 min (ca. 10% of FA was left in solution); the corresponding linear decays lasted for ca. 75 min for acetic acid (15% left), 30 min for propanoic acid (43% remaining), 45 min for butanoic acid (43% left), and 60 min for valeric acid (37% left in solution). Accordingly, the degradation process followed zero-order kinetics initially drifting toward first order at longer irradiation times. The relevant zero-order rates of degradation are summarized in Table 2.

Except for acetic acid, which was more refractory to oxidation than propanoic acid, a decreasing trend was seen in the rate of degradation with increasing chain length. Various factors can impact on the dynamics of the process occurring on TiO_2. The pH of a solution and the degree of adsorption of an acid on TiO_2 are intrinsically related.

The dark adsorption data (Fig. 1b; high catalyst load of 20 g/L) displayed no significant differences for the C2–C5 linear acids contrary to the rates of disappearance of these acids which are otherwise different. The extent of dark adsorption does not correlate with the rates of degradation. Hence, factors other than dark adsorption must play an important role in the degradation dynamics. Nonetheless, adsorption of the substrate on TiO_2 surface remains a relevant

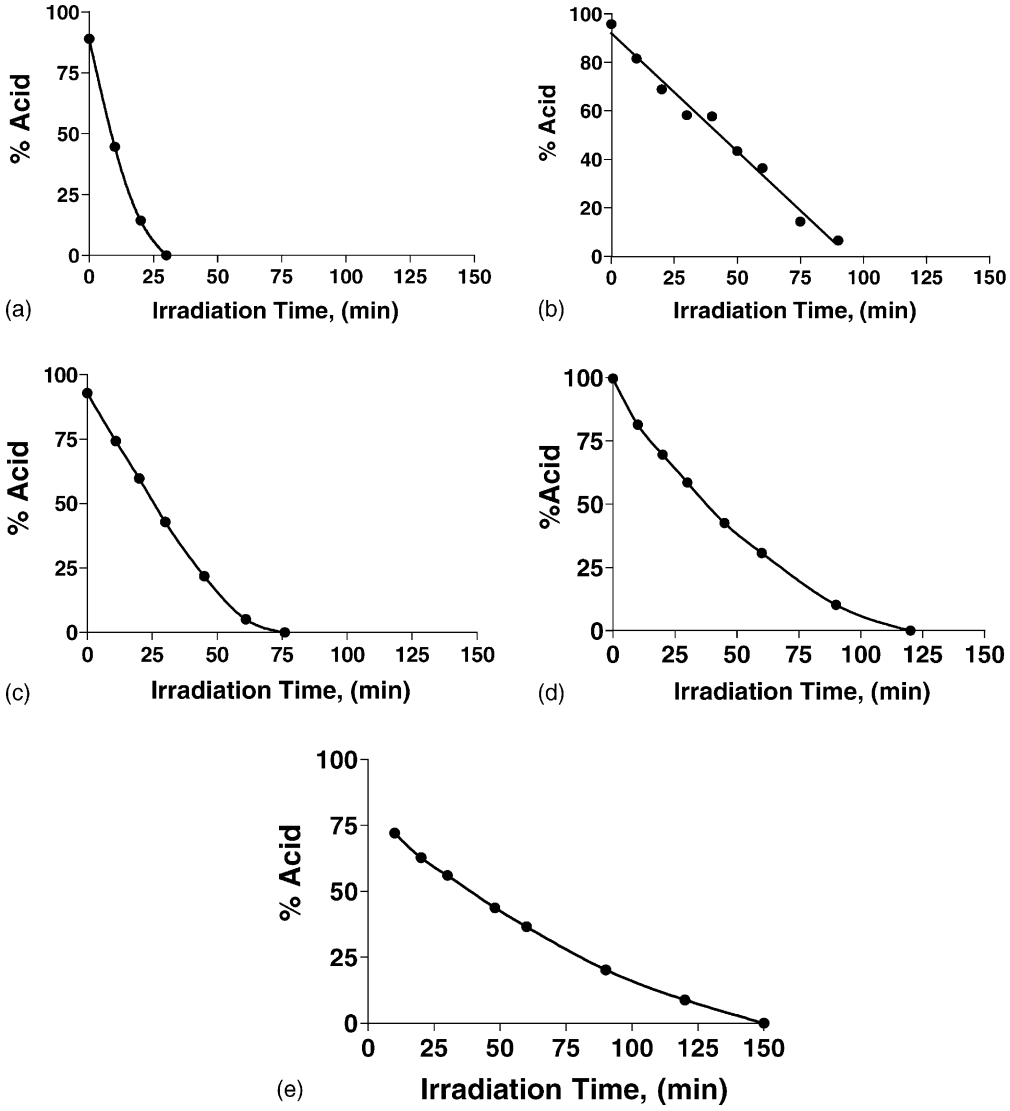

Fig. 4. Temporal changes in the concentration of the C1–C5 linear acids (normalized as percentage of initial concentration, 2.0×10^{-3} M) in air-equilibrated aqueous TiO_2 suspensions (catalyst loading, 2.0 g/L): (a) formic acid; (b) acetic acid; (c) propanoic acid; (d) butanoic acid; (e) valeric acid.

Table 2
Zero-order rate data for the degradation of the C1–C5 linear carboxylic acid series and rate of loss of TOC during the degradation of these acids

Acid	Rate of degradation (μmol/h)	Rate of TOC loss (mg/h)	Rate of TOC loss per C atom (mg/h)
Formic (FA)	238 ± 26 (224±25)[a]	2.9 ± 0.2	2.9 ± 0.2
Acetic (AA)	60 ± 4	1.30 ± 0.03	0.65 ± 0.03
Propanoic (PA)	100 ± 0.5	1.8 ± 0.1	0.60 ± 0.10
Butanoic (BA)	55 ± 2	1.22 ± 0.01	0.31 ± 0.01
Valeric (VA)	42 ± 2 (45±4)[a]	1.30 ± 0.03	0.26 ± 0.03

[a] Performed after one month illustrating the reproducibility of the methods used.

factor since the C2–C5 acids adsorbed less on TiO_2 than formic acid. The latter showed the highest rate of degradation (Table 2).

Changes in oxidative power of the valence band (VB) of UV-irradiated TiO_2 with pH are well-documented [8]. Band positions shift to more reducing potentials as pH increases, thus permitting manipulation of the redox chemistry using the pH factor. The bandgap however remains invariant to such pH changes. Among the C1–C5 acids, formic acid has the lowest pK_a and the lowest pH of the reaction medium. Consequently, the VB of TiO_2 is at a more positive redox potential in HCOOH/TiO_2 dispersions than is otherwise the case for the other C2−C5 acids that possess nearly identical pK_a's (see above), thereby causing TiO_2 to be a stronger oxidant with formic acid than with the other four acids. Moreover, formic acid is the better reducing agent of this linear acid series $\{E^\circ\ HCOO^-/HCOO^\bullet = -1.07\ V\ (NHE)\}$. Accordingly, the faster degradation of formic acid rests on three points: (1) adsorption in the dark on TiO_2 is greater than any of the other four acids; (2) formic acid is a stronger reducing agent; and (3) the pH of the solution was lowest causing irradiated TiO_2 to be a somewhat better oxidant. Thus, the degradation of formic acid is thermodynamically more favored relative to the other C2−C5 acids. Redox potentials and adsorption characteristics therefore impact on the rates of degradation of these acids [29–32].

The temporal decrease of TOC for the five acids under consideration is shown in Fig. 5. Near zero-order kinetics were observed for all acids in agreement with the work of Serpone et al. [33] and Tinucci and co-workers [34]. TOC decay patterns for butanoic acid and valeric acid display a small induction period initially (ca. 20 and 30 min, respectively),

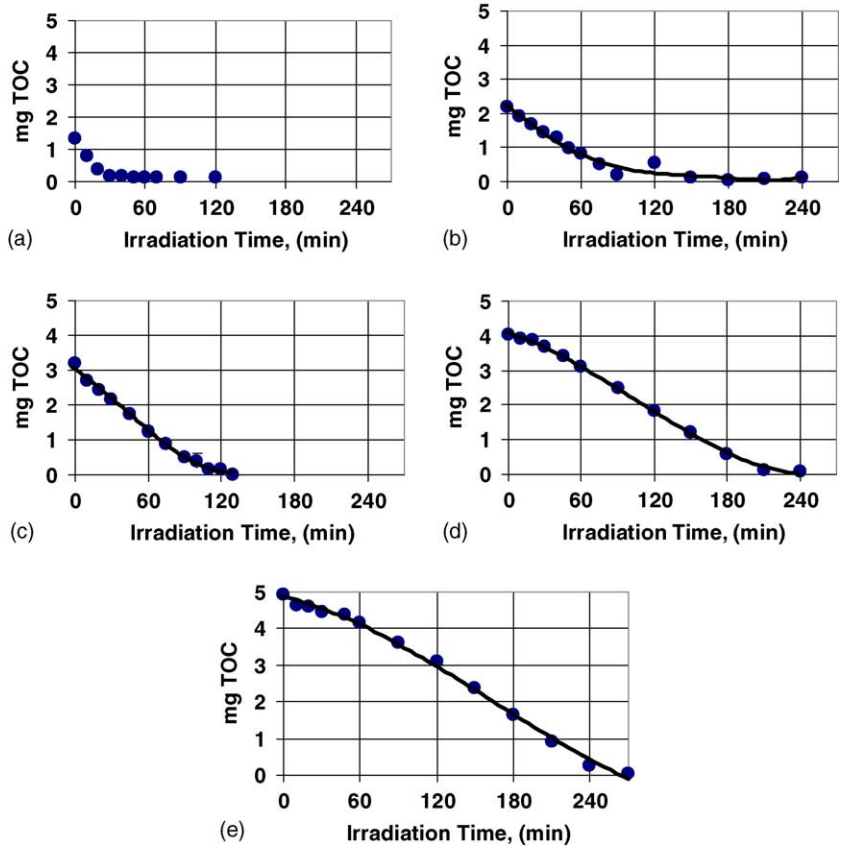

Fig. 5. Temporal changes in the concentration of TOC during the degradation of the C1–C5 linear acids (expressed as mg of TOC) in air-equilibrated aqueous TiO_2 suspensions (catalyst loading, 2.0 g/L): (a) formic acid; (b) acetic acid; (c) propanoic acid; (d) butanoic acid; (e) valeric acid.

attributed to formation of kinetically important intermediate species during the reaction. A substantial fraction of the total mineralization period is taken up by further oxidation of these intermediates. The incubation period increases with increasing solute concentration as a result of competition between degradation of intermediates and original substrate for the photogenerated •OH radicals [33,35]. Oxidation of formic acid led to its direct conversion to CO_2. In line with these observations, the degradation of formic acid and acetic acid produced no significant intermediates under our experimental conditions. An incremental number of intermediates were observed for the other C3–C5 acids (see below). Rate data for loss of TOC are summarized in Table 2.

The overall trend in the rates of TOC loss appears at variance with that observed for the rates of acid degradation (HPLC data). Formic acid displayed the highest rates of TOC loss and degradation. Unlike the rates of acid disappearance, however, which decreased with increasing chain length, the rates of TOC loss showed no particular trend. For example, there is little difference between butanoic acid and valeric acid. The rate of degradation of acetic acid was slightly greater than those of butanoic acid and valeric acid (Table 2). By comparison, the initial rates of TOC disappearance for these three acids were similar. However, the rate of TOC loss on a per carbon basis shows a decreasing trend with increase in chain length. There is no significant difference between rates of TOC loss and rates of acid degradation for the C1 and C2 acids, whereas the rates of TOC loss were lower than the rates of acid degradation for the C3–C5 acids.

Fig. 6 compares rates of TOC loss and rates of degradation of acetic acid (Fig. 6a) and butanoic acid (Fig. 6b) in terms of: (1) the temporal changes in percent TOC removed from solution; (2) the temporal changes in percent acid left in solution; and (3) the mass balance. The mass balance for acetic acid was nearly 100% at all sampling points, in line with no significant intermediates formed during degradation. For butanoic acid, the concentration of BA in solution decreased while the percent TOC removed increased, indicating a certain proportion of the acid had undergone complete mineralization. However, though the mass balance was 100% initially, it deviated negatively from 100% until a minimal value that corresponded to the complete disappearance of this acid. This infers an accumulation of carbon-containing intermediates that accompanied the disappearance of the original substrate, following which the intermediates were also photomineralized as evidenced by the rise in percent TOC removed from solution, albeit it was slightly below 100% after 210 min of irradiation.

TOC loss reflects a sum of exponential decays to which only the slower decay contributes most significantly [34]. Hence, TOC analyses are useful in evaluating the effectiveness of TiO_2 photocatalysis as a water treatment technology because it focuses on the complete mineralization of organic contaminants, including the intermediates. Note, however, that the TOC analysis is a non-specific method that provides no substrate-specific physical characteristics to the observed rates since they are not associated with a specific entity.

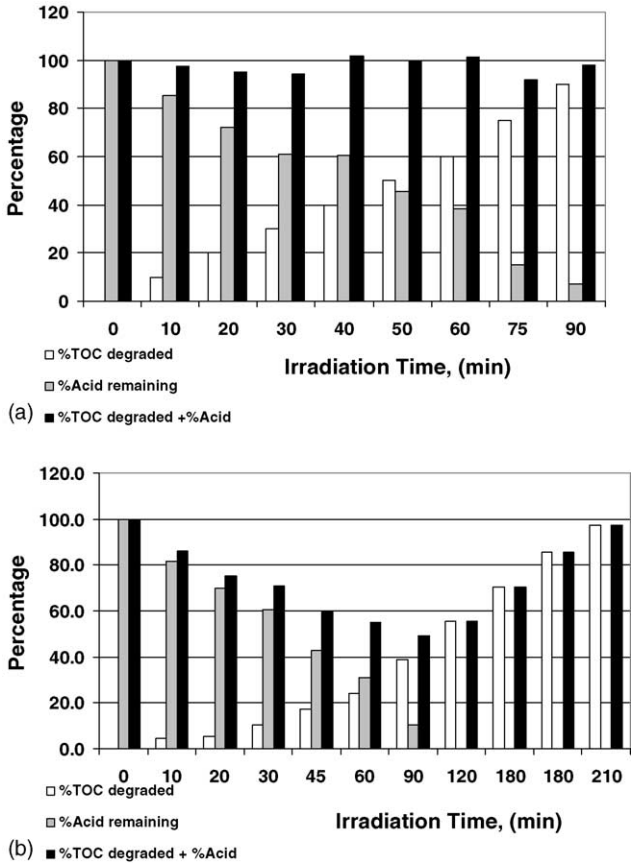

Fig. 6. (a) Histograms showing the percent of TOC decayed (left), the percent of acetic acid remaining in solution (middle) and the mass balance (right; expressed as %TOC degraded + %acid remaining) at various irradiation times. (b) Histograms showing the percent of TOC decayed (left), the percent of butanoic acid remaining in solution (middle) and the mass balance (right; expressed as %TOC degraded + %acid remaining) at various irradiation times. Note the negative curvature in (b) indicating substantive quantities of intermediates contrary to (a) for acetic acid for which intermediates were limited or non-existent.

3.5. Identification of oxidized intermediates

3.5.1. HPLC co-elution method

Hydrogen atoms on the α-carbon of the acids are the most labile hydrogens so that the α-carbon should be the preferred site for H-atom abstraction by •OH radicals, which in turn lead to formation of α-hydroxylated acids that can be oxidized further to α-keto derivatives.

The results were somewhat deceiving with respect to the above expectations except for 2-hydroxybutanoic acid identified as an intermediate of valeric acid degradation together with AA, PA, BA, and acrylic acid (HPLC co-elution method). Acetic acid was also an intermediate in the degradation of propanoic acid. In no other cases were α-hydroxy

acids or α-keto acids identified as intermediates by the co-elution method (but see below). However, since the rates of degradation of α-hydroxy and α-keto acids tend to be five-fold faster than those of the parent substrate [16], it is not surprising that such intermediates failed to be identified by co-elution. This is consistent with previous studies by Minero and co-workers [27] who reported that dodecyl derivatives (1-dodecanol and dodecanoic acid) are degraded rapidly at rates nearly 100-fold faster than dodecane, and that CO_2 is evolved almost at the same rate as dodecane degradation. Others [25] reported the first step in the photocatalyzed degradation of acetic acid involving surface-bound $^{\bullet}OH$ radicals abstracting a α-H to yield glycolate ($HOCH_2COO^-$) and glyoxylate ($OCHCOO^-$) species, contrary to other photocatalytic studies [27] involving acetic, propanoic and butanoic acid, which showed no formation of α-hydroxy or α-keto acids. Rather, aldehydes, ketones and alcohols were produced along with other carboxylic acids of different chain lengths. Variations with the present study reside in the otherwise different experimental conditions used.

3.5.2. GC–FID identification of valeric acid intermediates

Intermediates from valeric acid degradation were investigated further by GC–FID for confirmatory evidence. The intermediates in the degraded solution were extracted from aqueous media using diethyl ether, derivatized (carboxylic acids do not elute well on a GC column) and analyzed by gas chromatography. Both 2-oxovaleric acid (2-KVA), and 2-hydroxyvaleric acid (2-HVA) were included in this study to assess whether α-hydroxy and α-keto species were primary intermediates in the degradation of aliphatic linear acids. Valeric and butanoic acids were completely recovered from the aqueous sample after three extractions; recovery of 2-oxovaleric acid and 2-hydroxyvaleric acid was 87 and 62%, respectively. All four derivatized acids (VA, BA, 2-HVA and 2-KVA) were detected with appreciable signal intensities. Comparison of the chromatograms of the blank and the derivatized irradiated solution showed four peaks at shorter retention times than valeric acid, and 13 other peaks at longer retention times. With the type of column used (polysiloxane DB-5, 5% phenyl: 95% methyl), the elution order was expected to scale with the molecular weights of the species.

Except for acrylic acid, retention times of the linear acids followed the order: AA < PA < BA < VA, paralleling the molecular weights of the derivatized forms (133, 146, 160, and 174 g/mol, respectively). For oxidized and non-oxidized acids, the elution order was: linear < 2-oxo < 2-hydroxy. For example, the elution order of the C3 acids was: PA < 2-KPA < 2-HPA (146, 162, and 232 g/mol, respectively). Formic acid and acetic acid failed to be detected by this method. Formic acid was not detected by HPLC either, and acetic acid could not be confirmed by GC–FID. Butanol (and alcohols in general) was difficult to detect by HPLC because of its hydrophilicity and the lack of a chromophore absorbing at 214 nm. However, alcohols formed during the degradation of valeric acid were more likely to be detected by GC–FID. Thus, the greater number of peaks observed in the GC–FID chromatogram of a derivatized sample from the degraded valeric acid solution than in a HPLC chromatogram.

Combining the results from the HPLC and GC–FID analyses shows that the HPLC technique identified five valeric acid intermediates (AA, PA, BA, 2-HBA, and acrylic acid), whereas four valeric acid intermediates (PA, BA, 2-HBA, and 2-KBA) were identified by GC–FID. Three were simultaneously identified by the two methods (PA, BA, and 2-HBA). Clearly, an α-hydroxyacid (2-HBA) was formally identified, indicating the occurrence of hydroxylation at the α-carbon.

3.5.3. Identification of valeric acid intermediates by GC–MS methods

Sample handling for GC–MS analyses was identical to that used for GC–FID, except that the extraction was carried out on the whole 400 mL of the filtrate from irradiated dispersions instead of the 60 mL aliquot. This led to the recovery of larger quantities of intermediates. The derivatized filtrate was analyzed by GC–FID prior to performing GC–MS analyses to optimize the separation method. More than 40 peaks were detected in the GC–FID chromatogram with the scaled-up extraction procedure, as opposed to 17 with the former method, thus adding a further challenge in identifying intermediates even for a simple linear aliphatic acid.

Species identified by the GC–MS methodology are summarized in Table 3. Most intermediates formed in the photocatalytic degradation of valeric acid are saturated aliphatic acids with shorter chain length. The presence of 2-methylbutanoic acid, 2-methylmalonic acid and hexanoic acid indicates addition of alkyl groups on the main carbon backbone. The remaining intermediates were: (1) saturated and unsaturated hydroxyacids {4-HBA, 3-HVA, 4-HVA acid, 5-HVA, and 2-hydroxy-2-pentenoic acid}; (2) saturated ketoacids {4-KVA}; and (3) saturated and unsaturated diacids {succinic acid, 2-methylmalonic acid, and 1-propene-1,3-dicarboxylic acid}. The presence of 2-hydroxy-2-pentenoic acid also points to hydroxylation on the α-carbon of valeric acid. Note that 2-hydroxyvaleric acid was detected neither by HPLC nor by GC–FID methods. However, hydroxylation did take place on carbon atoms other than the α-carbon, as evidenced by formation of 3-hydroxy, 4-hydroxy, and 5-hydroxyvaleric acid as well as 2-hydroxy-2-pentenoic acid. Hydroxyacids undergo further oxidation to the keto (oxo) species, as indicated by the presence of 4-oxovaleric acid. The presence of dicarboxylic acids (succinic acid, 2-methylmalonic acid, and 1-propene-1,3-dicarboxylic acid) is not surprising given that hydroxyacids were produced with the hydroxyl group located on terminal carbon atoms at which further oxidation yields a carboxyl group.

Table 4 shows the results obtained by the three analytical methods used to identify some of the intermediates produced in the degradation of valeric acid. Only butanoic acid and 2-hydroxybutanoic acid were confirmed by all three methods. Propanoic acid was positively identified by HPLC

Table 3
Final results of the GC–MS investigation of the intermediates of valeric acid (see text and for details regarding interpretation of this table)

Derivatized acids (esters)	General formula	Correlated acid	Retention times (r.t., min)
Trimethylsilylbutanoate	$C_7H_{16}SiO_2$	Butanoic acid	6.22
Trimethylsilyl-2-methylbutanoate	$C_8H_{18}SiO_2$	2-Methylbutanoic acid	6.28
Trimethylsilylpentanoate	$C_8H_{18}SiO_2$	Valeric acid	6.60
Trimethylsilyl-2-[oxo(trimethylsilyl)]butanoate[a]	*$C_{10}H_{24}Si_2O_3$*	*2-Hydroxybutanoic acid*	*6.85*
Trimethylsilyl-4-oxopentanoate	$C_8H_{16}SiO_3$	4-Oxovaleric acid	7.45
Trimethylsilyl-2-methyl-2-[(trimethylsilyl)oxo]-propanoate[a]	*$C_{10}H_{24}Si_2O_3$*	*2-Hydroxy-2-methylpropanoic acid*	*7.56*
(2-Methoxy-ethoxy)-trimethylsilane[a]	*$C_6H_{16}SiO_2$*	*2-Methoxy-ethanol*	*7.83*
Trimethylsilyl-2-[(trimethylsilyl)oxo]-2-pentenoate[a,b]	*$C_{11}H_{24}Si_2O_3$*	*2-Hydroxy-2-pentenoic acid*	*7.91*
Trimethylsilyl-4-[oxo(trimethylsilyl)]butanoate	$C_{10}H_{21}Si_2O_3$	4-Hydroxybutanoic acid	7.97
Trimethylsilyl-4-[oxo(trimethylsilyl)]pentanoate	$C_{11}H_{25}Si_2O_3$	4-Hydroxyvaleric acid	8.09
Trimethylsilyl-2-[oxo(trimethylsilyl)]-2-pentenoate [b]	$C_{11}H_{24}Si_2O_3$	2-Hydroxy-2-pentenoic acid	8.18
Trimethylsilyl-3-[oxo(trimethylsilyl)]pentanoate	$C_{11}H_{24}Si_2O_3$	3-Hydroxyvaleric acid	8.24
bis(Trimethylsilyl)succinate	$C_{10}H_{22}Si_2O_4$	Succinic acid	8.37
Trimethylsilyl-5-[oxo(trimethylsilyl)]pentanoate	$C_{11}H_{26}Si_2O_3$	5-Hydroxyvaleric acid	8.45
bis(Trimethylsilyl)malonate[a]	*$C_9H_{20}Si_2O_4$*	*Malonic acid*	*8.77*
bis(Trimethylsilyl)-1-propene-1,3-dicarboxylate	$C_{11}H_{22}Si_2O_4$	1-Propene-1,3-dicarboxylic acid	8.85
bis(Trimethylsilyl)-2-methyl-malonate	$C_{10}H_{22}Si_2O_4$	2-Methyl-malonic acid	9.82
Trimethylsilylhexanoate[a]	*$C_9H_{20}SiO_2$*	*Hexanoic acid*	*9.91*

[a] The molecular weights of these intermediates did not follow the correlation with retention times (see text).
[b] This species (r.t. = 7.91 min) was matched to a mass spectrum in the mass spectral library to a 60% level, in contrast to the intermediate with r.t. = 8.81 min, which was 90% matched to 2-hydroxy-2-pentenoic acid. Also note that this species is the enol form of 2-oxovaleric acid. However, the latter could not be derivatized under our conditons, and thus was not detected.

Table 4
Combined HPLC–UV, GC–FID, and GC–MS results for the identification of the intermediates of valeric acid (in bold, identified species; see Scheme 1)

Number of the intermediate	Acid	Positive ID by HPLC	Positive ID by GC–FID	Positive ID by GC–MS
17	{Formic}	(Yes)[a]	No	No
14	**Acetic**	**Yes**	No	No
**	*Hydroxyacetic*	*No*	*No*	*No*
9	**Propanoic**	**Yes**	**Yes**	No
**	*2-Hydroxypropanoic*	*No*	*No*	*No*
**	*2-Oxopropanoic*	*No*	*No*	*No*
13	**2-Methylmalonic**	[b]	[b]	**Yes**
6	**Butanoic**	**Yes**	**Yes**	**Yes**
11	**2-Hydroxybutanoic**	**Yes**	**Yes**	**Yes**
12	**4-Hydroxybutanoic**	[b]	[b]	**Yes**
15	**2-Oxobutanoic**	No	**Yes**	No
10	**2-Methylbutanoic**	[b]	[b]	**Yes**
16	**Succinic**	[b]	[b]	**Yes**
[c]	*2-Oxosuccinic*	No	No	No
18	**Acrylic**	Yes	No	No
[c]	*2-Oxovaleric*	*No*	*No*	*No*
[c]	*2-Hydroxyvaleric*	*No*	*No*	*No*
4	**3-Hydroxyvaleric**	[b]	[b]	**Yes**
3	**4-Hydroxyvaleric**	[b]	[b]	**Yes**
7	**4-Oxovaleric**	[b]	[b]	**Yes**
2	**5-Hydroxyvaleric**	[b]	[b]	**Yes**
8	**2-Hydroxy-2-pentenoic acid**	[b]	[b]	**Yes**
5	**1-Propene-1,3-dicarboxylic**	[b]	[b]	**Yes**
19	**Hexanoic**	[b]	[b]	**Yes**
20	**2-Hydroxy-2-methyl propanoic**	[b]	[b]	**Yes**
21	**Malonic**	[b]	[b]	**Yes**

[a] Eluted in the solvent front.
[b] Not examined by GC–FID or by HPLC co-elution methods.
[c] These intermediates were identified by none of the three analytical methods used.

and GC–FID but not by GC–MS, because the derivatized propanoic acid eluted with the solvent front. Nonetheless, the evidence indicates that hydroxylation and alkylation of the carbon backbone of these aliphatic acids occurred, that compounds with less carbon atoms were formed, and that an oxidative process also led to some unsaturated compounds.

3.6. Mechanism of degradation

3.6.1. Partial charges and frontier electron densities

Table 5 summarizes the partial charges and frontier electron densities of all atoms of the five C1–C5 linear aliphatic acids (those of the H atoms are not listed but were included in the calculations). Except for the C^1 carbon of the carboxylic acid function, all other carbons carry a partial negative charge with the highest charge born by the terminal methyl carbon. Accordingly, the acids not only adsorb to the TiO_2 particle through the carboxylate oxygens, but to some extent also through the hydrocarbon chain when the surface is positively charged. This infers that the acids may also adsorb horizontally along the surface.

Table 5
Partial charges and frontier electron densities of atoms in the C1–C5 linear aliphatic carboxylic acids (note that the H atoms were also included in the calculations, but are not reported below)

Atoms	Partial charge	Electron density
$H–C^{1}(=O^{2})–O^{1}–H$		
C1	0.369	0.756
O1	−0.376	0.283
O2	−0.535	0.855
$H_3C^{2}–C^{1}(=O^{2})–O^{1}–H$		
C1	0.404	0.682
C2	−0.244	0.108
O1	−0.354	0.237
O2	−0.531	0.877
$H_3C^{3}–C^{2}H_2–C^{1}(=O^{2})–O^{1}–H$		
C1	0.396	0.680
C2	−0.175	0.159
C3	−0.222	0.136
O1	−0.357	0.154
O2	−0.516	0.537
$H_3C^{4}–C^{3}H_2–C^{2}H_2–C^{1}(=O^{2})–O^{1}–H$		
C1	0.399	0.655
C2	−0.177	0.099
C3	−0.159	0.191
C4	−0. 224	0.117
O1	−0.357	0.107
O2	−0.514	0.337
$H_3C^{5}–C^{4}H_2–C^{3}H_2–C^{2}H_2–C^{1}(=O^{2})–O^{1}–H$		
C1	0.398	0.653
C2	−0.177	0.049
C3	−0.158	0.133
C4	−0.163	0.171
C5	−0.222	0.085
O1	−0.357	0.092
O2	−0.514	0.281

The frontier electron density on the α-carbon atoms of the C4 and C5 linear acids (i.e. the C^2 carbons) is lowest relative to the other carbon atoms in the chain. Thus, $^{\bullet}$OH radical attack at these α-carbons is not expected to be the predominant step, as evidenced experimentally by the failure to detect 2-hydroxyvaleric acid. By contrast, the electron density on the α-carbon of butanoic acid is two-fold greater than for the α-carbon of valeric acid. Indeed, 2-hydroxybutanoic acid was an intermediate identified in the degradation of butanoic acid by HPLC co-elution and GC–FID techniques (Table 4). In the case of valeric acid, the electron densities are significant such that hydroxylation of the C^3, C^4 and C^5 carbons of this C5 linear acid is not unexpected. Experimentally, this expectation was realized as the corresponding hydroxylated intermediates 3-hydroxy, 4-hydroxy and 5-hydroxyvaleric acids were positively identified in the photodegradation of valeric acid (Table 4). Only the 4-hydroxybutanoic acid was identified under our conditions, albeit in the degradation of valeric acid.

3.6.2. Suggested pathway of valeric acid degradation

On the basis of the above evidence, Scheme 1 accounts, at least in part, for the species formed in the photodegradation of valeric acid (**1**) and its smaller congeners. Intermediate **3** (4-hydroxyvaleric acid) arises from attack of a $^{\bullet}$OH radical on the C^4 carbon atom of valeric acid, generating a secondary radical intermediate that further reacts with surface-bound $\{^{\bullet}OH/H_2O\}$ species, or some other reactive oxygen species, to yield 4-hydroxyvaleric acid (Eq. (1)).

$$CH_3CH_2CH_2CH_2COOH_{(ads)} + {}^{\bullet}OH_{(ads)} \rightarrow CH_3C^{\bullet}HCH_2CH_2COOH_{(ads)} + H_2O \quad (1a)$$

$$CH_3C^{\bullet}HCH_2CH_2COOH_{(ads)} + \{^{\bullet}OH/H_2O\}_{(ads)} \rightarrow CH_3CH(OH)CH_2CH_2COOH_{(aq)} \quad (1b)$$

Similarly, intermediate **4** (3-HVA, Eq. (2)) and intermediate **2** (5-HVA, Eq. (3)) are formed by an analogous route.

$$CH_3CH_2CH_2CH_2COOH_{(ads)} + {}^{\bullet}OH_{(ads)} \rightarrow CH_3CH_2C^{\bullet}HCH_2COOH_{(ads)} + H_2O \quad (2a)$$

$$CH_3CH_2C^{\bullet}H\,CH_2COOH_{(ads)} + \{^{\bullet}OH/H_2O\}_{(ads)} \rightarrow CH_3CH_2CH(OH)CH_2COOH_{(aq)} \quad (2b)$$

$$CH_3CH_2CH_2CH_2COOH_{(ads)} + {}^{\bullet}OH_{(ads)} \rightarrow {}^{\bullet}CH_2CH_2CH_2CH_2COOH_{(ads)} + H_2O \quad (3a)$$

$${}^{\bullet}CH_2CH_2CH_2CH_2COOH_{(ads)} + \{^{\bullet}OH/H_2O\}_{(ads)} \rightarrow HOCH_2CH_2CH_2CH_2COOH_{(aq)} \quad (3b)$$

Hydroxylation on the C^3, C^4 and C^5 carbon atoms of valeric acid did occur. We infer that valeric acid adsorbed on

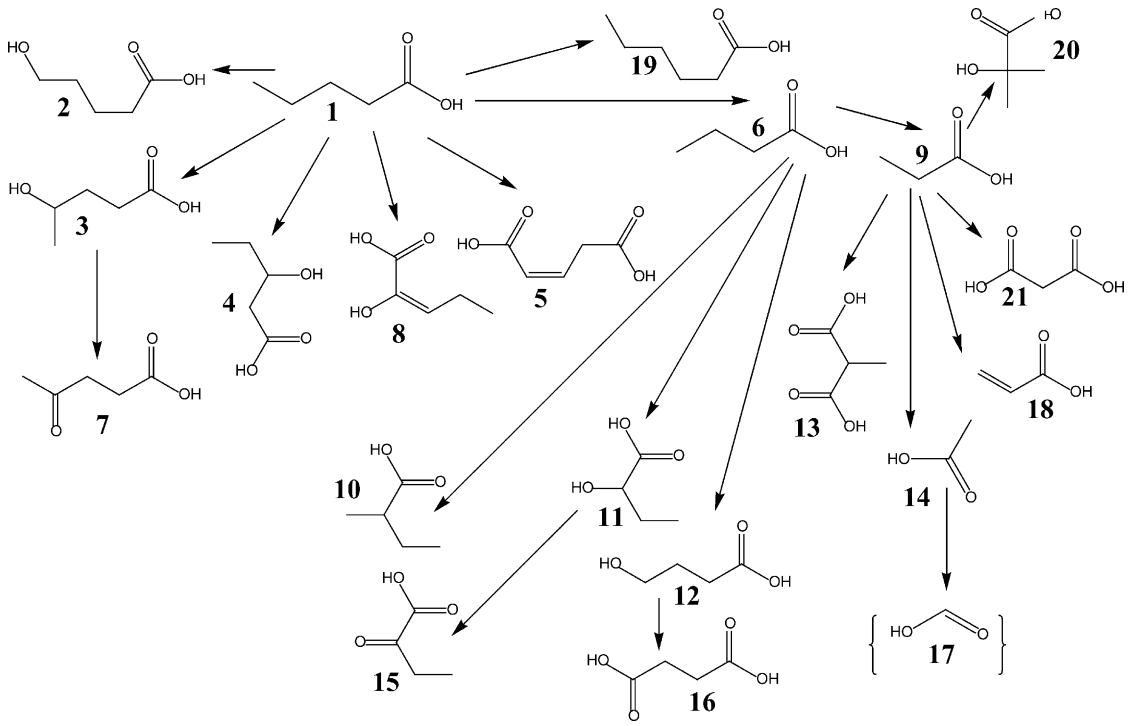

Scheme 1. Proposed origins of intermediates identified in the TiO_2 photocatalyzed degradation of valeric acid based on results from HPLC co-elution, GC–FID relative retention times, and GC–MS analyses of the degraded solution of valeric acid in an air-equilibrated UV-irradiated TiO_2 dispersion. The presence of intermediates **10**, **13** and **19** indicate that methylation of the precursor takes place by combination of the appropriate precursor radical with methyl radicals from the $^{\bullet}OH$ radical oxidative decarboxylation of acetic acid (Eq. (10)).

TiO_2 allowing the hydrophobic chain to be in close proximity to an otherwise hydrophilic surface and thus in close proximity to surface-bound $^{\bullet}OH$ radicals. This hypothesis finds support in the occurrence of intermediates **5** and **8** (1-propene-1,3-dicarboxylic acid and 2-hydroxy-2-pentenoic acid) and from the partial charge data of Table 5. Such olefinic acids are likely formed by hydroxylation of valeric acid followed by dehydrogenation before desorbing from the catalyst surface. Intermediate **7** (4-KVA) is a secondary intermediate originating from oxidation of 4-hydroxyvaleric acid (intermediate **3**) since alcohols can adsorb on TiO_2 forming alkoxides [36]. A similar path would take intermediate **11** to the oxidized species **15** (2-KBA).

Shorter chain length acids also formed in the degradation of valeric acid: butanoic acid (**6**), propanoic acid (**9**) and acetic acid (**14**). These acids originated from reaction of valeric acid with a photogenerated trapped hole in TiO_2 ($\{h^+/Ti^{IV}-{}^{\bullet}OH\}$; Eq. 4a) followed by decarboxylation of the carboxylate radical intermediate evolving CO_2 and an alkyl radical (Eq. (4b)). Further reaction

$$CH_3CH_2CH_2CH_2COOH_{(ads)} + \{h^+/Ti^{IV} - {}^{\bullet}OH\}_{(ads)} \rightarrow CH_3CH_2CH_2CH_2COO^{\bullet} + TiO_2 + H^+ \quad (4a)$$

$$CH_3CH_2CH_2CH_2COO^{\bullet}{}_{(ads)} \rightarrow (CH_3CH_2CH_2C^{\bullet}H_2 + CO_2 \quad (4b)$$

$$CH_3CH_2CH_2C^{\bullet}H_2 + \{{}^{\bullet}OH/H_2O\}_{(ads)} \rightarrow CH_3CH_2CH_2CH_2OH_{(aq)} \quad (4c)$$

converted the radical to an alcohol. Subsequent similar oxidation steps led to butanoic acid. The process can repeat itself to yield propanoic acid and acetic acid.

The demonstration that the rate at which $^{\bullet}OH$ radicals oxidize similar compounds is less than the rate at which $^{\bullet}OH$ radicals combine with dissolved oxygen [10] suggests an alternative but equally valid pathway (the Russell mechanism). In this case, the mechanism by which valeric acid converts to butanoic acid involves initial photocatalyzed decarboxylation to give the alkyl radical species (Eqs. (4a) and (4b)), which then reacts with O_2 to form a peroxy radical (Eq. (5)). In turn, this radical combines with $^{\bullet}OOH$ (formed through protonation of the superoxide radical anion, $O_2{}^{\bullet-}$) to yield the unstable tetroxide species (Eq. (6)) followed by its decomposition to an aldehyde, water, and

$$CH_3CH_2CH_2C^{\bullet}H_{2(ads)} + O_{2(ads)} \rightarrow CH_3CH_2CH_2CH_2{-}O{-}O^{\bullet} \quad (5)$$

$$CH_3CH_2CH_2CH_2{-}O{-}O^{\bullet} + {}^{\bullet}OOH \rightarrow CH_3CH_2CH_2CH_2OOOOH \quad (6)$$

$$CH_3CH_2CH_2CH_2OOOOH \rightarrow CH_3CH_2CH_2CHO + H_2O + O_2 \quad (7)$$

oxygen (Eq. (7)). In the former route (Eq. (4)), formation of a shorter chain involved formation of an alcohol and

an aldehyde. None of these compounds were detected by GC–MS. The Russell pathway for valeric acid would lead to an aldehyde that is further oxidized to an acid. Note, however, that aldehydes and ketones are not derivatized by the procedure used. For instance, given the high volatility of butanal (if formed) it would have eluted with the solvent front, as would have shorter chain aldehydes, and consequently would not have been detected by the analytical procedures employed. As well, butanol would not have been recovered from an irradiated valeric acid/TiO_2 suspension even with the scaled-up extraction procedure because of its high water solubility. The derivatized butanol derivative {$CH_3CH_2CH_2CH_2$–$OSi(CH_3)_3$; molecular weight, 146 g/mol} would also have eluted with the solvent front. Consequently, numerous intermediates went undetected.

The alkylated compounds 2-methylbutanoic acid {(**10**); Scheme 1; Eqs. (8) and (9)}, 2-methyl-malonic acid (**13**), and hexanoic acid (Table 4) are formed following recombination of two alkyl

$$CH_3CH_2CH_2COOH_{(ads)} + {}^{\bullet}OH_{(ads)} \rightarrow CH_3CH_2C^{\bullet}HCOOH_{(ads)} + H_2O \quad (8)$$

$$CH_3CH_2C^{\bullet}HCOOH_{(ads)} + {}^{\bullet}CH_3 \rightarrow CH_3CH_2CH(CH_3)COOH_{(aq)} \quad (9)$$

radicals. The methyl radical likely originated from the decarboxylation of acetic acid (Eq. (10)), an intermediate product of valeric acid degradation.

$$CH_3COOH + {}^{\bullet}OH_{(ads)} \xrightarrow{-H^+} CH_3COO^{\bullet} \rightarrow {}^{\bullet}CH_3 + CO_2 \quad (10)$$

3.7. Limiting photonic efficiency of formic acid and quantum yields of degradation of the C1–C5 acids

Formic acid was chosen as the standard molecule (secondary actinometer) with which to compare process efficiencies of other aliphatics because results of the TiO_2 photocatalyzed degradation indicated no significant intermediates formed. Also, the rate of degradation of formic acid (HPLC) was identical to the rate of loss of TOC confirming that no C-containing species accumulated in solution as degradation proceeded.

The quantum yield (Φ) of degradation of formic acid was determined from the limiting photonic efficiency (ξ_{lim}) at high TiO_2 loadings using the protocol proposed by Serpone and co-workers [18] who showed that under these conditions $\xi_{lim} = \Phi$. Hence, photonic efficiencies of AA, PA, BA, VA, and 2-MBA relative to formic acid (ξ_{rel}) can lead to estimates of Φ of photodegradation of other aliphatic acids, and aliphatics in general, since $\Phi_{acid} = \xi_{rel}\Phi_{standard}$.

The rate of degradation of formic acid reached a plateau at ca. 2.0×10^{-3} M above which the rates were no longer

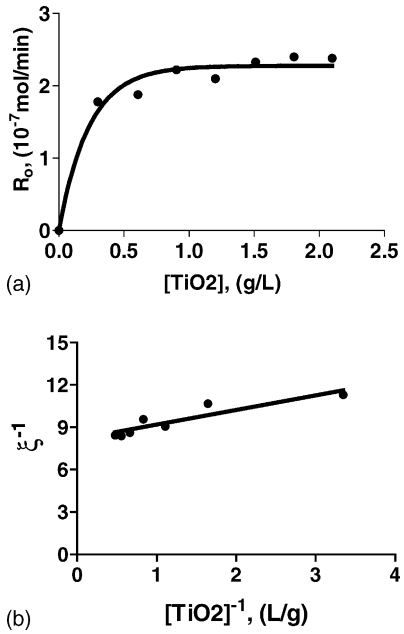

Fig. 7. (a) Plot of initial rates of degradation of formic acid for various loadings of TiO_2. (b) Double reciprocal plot of the photonic efficiency, ξ^{-1}, against TiO_2 loadings as $[TiO_2]^{-1}$ (see text for details).

concentration dependent. Also, the rates scaled linearly with photon flow (ρ; light irradiance). It is relevant to emphasize that these are two critical requirements that must be met to satisfy the definition of the quantum yield [18,37]: that is (a) Φ must be independent of concentration—hence the kinetics must be zero-order, and (b) the rates of degradation must scale linearly with photon flow, ρ. To satisfy the first criterion, the Φ of formic acid was determined at a concentration in HCOOH of 4.0×10^{-3} M. The initial zero-order rates obtained at various TiO_2 loadings (from 0.30 to 2.1 g/L) are plotted against TiO_2 loading in Fig. 7a. Aberchrome 540 was the chemical actinometer to establish the photon flow impinging on the reactor at 365 nm ($\rho = 2.01 \pm 0.26 \times 10^{-6}$ Einstein/min). Photonic efficiencies were estimated at various TiO_2 loadings as $\xi = R_0/\rho$, where R_0 is the zero-order rate of degradation. The double reciprocal plot of ξ^{-1} versus $[TiO_2]^{-1}$ illustrated in Fig. 7b gave [18] ξ_{lim} of formic acid as $0.12 \pm 0.02 = \Phi_{formic}$.

Acetic acid, propanoic acid, butanoic acid, valeric acid, and 2-methylbutanoic acid were degraded under otherwise identical conditions to those of formic acid. The relative photonic efficiencies and the quantum yields of degradation of these acids are listed in Table 6. Acetic acid displayed the lowest quantum yield of degradation; of the C1–C5 linear acid series it was also the slowest to degrade. Quantum yields increase from acetic acid to valeric acid, paralleling the increase in chain length. Methylation of butanoic acid seems to have had no effect on Φ of degradation—e.g. compare butanoic acid and 2-methylbutanoic acid ($\Phi = 0.37$ for both).

Table 6
Relative photonic efficiencies and quantum yields of degradation for selected acids using formic acid as a standard secondary actinometer (see ref. [18])

Acid	ξ_{rel}	$\Phi = \xi_{rel}\ \Phi_{formic}$
Formic (FA)	1.0	0.12 ± 0.02
Acetic (AA)	0.08 ± 0.01	0.010 ± 0.001
Propanoic (PA)	0.20 ± 0.03	0.024 ± 0.006
Butanoic (BA)	0.28 ± 0.06	0.037 ± 0.007
Valeric (VA)	0.56 ± 0.07	0.067 ± 0.008
2-Methylbutanoic (2-MBA)	0.31 ± 0.05	0.037 ± 0.006

4. Conclusions

In summary, the extent of dark adsorption of formic acid (34%) was two-old greater than for the other C2–C5 acids (15–19%) under otherwise identical experimental conditions (high TiO_2 catalyst load, 20 g/L; $[acid]_0$ 2.0×10^{-3} M; pH 3.7). All five C1–C5 linear acids were completely photodegraded and mineralized in UV-irradiated TiO_2 dispersions. Accordingly, TiO_2 photocatalysis is an attractive advanced oxidation technology to remove linear carboxylic acids and intermediates from aquatic media. A total of 21 intermediates were identified in the photocatalyzed degradation of valeric acid: (1) aliphatic saturated and unsaturated carboxylic acids and diacids with the same or shorter chain length than the parent compound, in addition to hexanoic acid; (2) methylated branched saturated aliphatic acids and diacids of shorter chain length than the parent compound; (3) saturated and unsaturated hydroxyacids of the same or shorter chain length than the parent compound; and (4) saturated oxoacids of the same or shorter chain length than the parent compound.

The intermediates 2-HVA and 2-KVA were not detected in the degradation of valeric acid. However, identification of 2-hydroxybutanoic acid and 1-propene-1,3-dicarboxylic acid indicates that hydroxylation can take place on the α-carbon of these acids. Failure to detect 2-HVA and 2-KVA is likely the result of the ease with which these species are further oxidized (by $^{\bullet}OH$ radicals or other reactive oxygen species); note also that 2-KVA could not be derivatized and thus detected. The presence of 5-hydroxy-, 4-hydroxy- and 3-hydroxyvaleric acids confirmed the hydroxylation of the carbon backbone of valeric acid in the degradation of this acid. As well, that the 4-hydroxyvaleric acid/4-oxovaleric acid and the 2-hydroxybutanoic acid/2-oxobutanoic acid couples are formed infers that once hydroxylated, the hydroxyl group is further oxidized to the keto function. All the compounds identified could be accounted by a mechanism that involved $^{\bullet}OH$ radicals and methyl radicals ((CH_3), which have been shown to form in the photocatalyzed degradation of carboxylic acids [8].

Finally, not all the compounds that formed during the photocatalytic degradation of valeric acid could be identified. The pathway leading to the degradation of a fairly simple compound such as valeric acid is rather complex yielding a broad spectrum of intermediates. The quantum yield of degradation of formic acid has been determined and is proposed as a means to determine the quantum yields of similar processes for several other aliphatics, in the same manner as phenol was proposed for aromatics [18].

Acknowledgements

This study was supported in part by a grant from the Natural Sciences and Engineering Research Council of Canada (to N.S.) and in part from the Ministero dell'Istruzione, dell'Università e della Ricerca (MIUR-Rome, Italy; to N.S.). Work carried out in Tokyo was sponsored by the Japanese Ministry of Education, Culture, Sports, Sciences and Technology (to H.H.).

References

[1] S.T. Cragg, Aliphatic carboxylic acids saturated, in: E. Bingham, B. Cohrssen, C.H. Powell (Eds.), Patty's Toxicology, fifth ed., Wiley, New York, 2001, pp. 689–787.
[2] D.L. Camper, G.H. Loew, J.R. Collins, Intern. J. Quantum Chem. Quantum Biol. Symp. 17 (1990) 173.
[3] C.J. Moudgal, J.C. Lipscomb, R.M. Bruce, Toxicology 147 (2000) 109.
[4] M.G. Narotsky, E.Z. Francis, R.J. Kavlock, Fund. Appl. Toxicol. 22 (1994) 251.
[5] L. Legal, B. Moulin, J.M. Jallon, Pestic. Biochem. Phyisol. 65 (1999) 90.
[6] C. Guillard, J. Photochem. Photobiol. A: Chem. 135 (2000) 63.
[7] Y. Inel, A.N. Okte, J. Photochem. Photobiol. A: Chem. 96 (1996) 175.
[8] T. Sakata, T. Kawai, K. Hashimoto, J. Phys. Chem. 88 (1984) 2344.
[9] H.L. Chum, M. Ratcliff, F.L. Posey, J.A. Turner, A.J. Nozik, J. Phys. Chem. 87 (1983) 3089.
[10] J. Schwitzgebel, J.G. Ekerdt, H. Gerisher, A. Heller, J. Phys. Chem. 95 (1999) 5633.
[11] M.I. Franch, J.A. Ayllon, J. Peral, X. Domenech, Catal. Today 76 (2002) 221.
[12] M. Sturini, F. Soana, A. Albini, Tetrahedron 58 (2002) 2943.
[13] N. Serpone, D. Lawless, R. Terzian, D. Meisel, Redox mechanisms in heterogeneous photocatalysis. The case of holes vs. $^{\bullet}OH$ radical oxidation and free vs. surface-bound $^{\bullet}OH$ radical oxidation processes, in: R. McKay, J. Texter (Eds.), Electrochemistry in Colloids and Dispersions, VCH Publishers, New York, 1992, pp. 399–416; D. Lawless, N. Serpone, D. Meisel, J. Phys. Chem. 95 (1991) 5166.
[14] N. Serpone, A.V. Emeline, Modeling heterogeneous photocatalysis by metal-oxide nanostructured semiconductor and insulator materials. Factors that affect the activity and selectivity of photocatalysts, Res. Chem. Intermed., in press;
A.V. Emeline, A. Frolov, V. Ryabchuk, N. Serpone, J. Phys. Chem. B 107 (2003) 7109.
[15] M.I. Franch, J.A. Ayllon, J. Peral, X. Domenech, Appl. Catal. B: Environ. 50 (2004) 89.
[16] N. Serpone, J. Martin, S. Horikoshi, H. Hidaka, J. Photochem. Photobiol. A: Chem., in press.
[17] Y. Mao, C. Schöneich, K.-D. Asmus, J. Phys. Chem. 95 (1991) 10080.
[18] A. Salinaro, A.V. Emeline, J. Zhao, H. Hidaka, V.K. Ryabchuk, N. Serpone, Terminology, relative photonic efficiencies and quantum yields in heterogeneous photocatalysis. Part II. Experimental determination of quantum yields, Pure Appl. Chem. 71 (1999) 321;

N. Serpone, A. Salinaro, Terminology, relative photonic efficiencies and quantum yields in heterogeneous photocatalysis. Part I. Suggested protocol, Pure Appl. Chem. 71 (1999) 303.
[19] N. Serpone, R.F. Khairutdinov, Studies Surf. Sci. Catal. 103 (1997) 417.
[20] K.S. Kim, M.A. Barteau, Langmuir 4 (1988) 945.
[21] J. Cunningham, P. Sedlak, Initial rates of TiO_2-photocatalyzed degradations of water pollutants: influences of adsorption, pH and photon-flux, in: D.F. Ollis, H. Al-Ekabi (Eds.), Photocatalytic Purification and Treatment of Water and Air, Elsevier, Amsterdam, 1993, pp. 67–81.
[22] P. Pichat, Photocatalysis: heterogeneous regime. Catalysts adsorption and the new techniques, in: E. Pelizzetti, M. Schiavello (Eds.), Photochemical Conversion and Storage of Solar Energy, Kluwer, The Netherlands, 1991, pp. 277–293.
[23] K. Nohara, H. Hidaka, E. Pelizzetti, N. Serpone, J. Photochem. Photobiol. A: Chem. 102 (1997) 265;
H. Hidaka, K. Nohara, J. Zhao, E. Pelizzetti, N. Serpone, J. Photochem. Photobiol. A: Chem. 91 (1995) 145.
[24] A. Mills, S. Le Hunte, J. Photochem. Photobiol. A: Chem. 108 (1997) 1.
[25] D. Bahnemann, J. Cunningham, M.A. Fox, E. Pelizzetti, P. Pichat, N. Serpone, Photocatalytic treatment of waters, in: G.R. Helz, R.G. Zepp, D.G. Crosby (Eds.), Aquatic and Surface Photochemistry, Lewis Publishers, Boca Raton, FL, 1994, pp. 261–316.
[26] P. Pichat, C. Guillard, L. Amalric, A.-C. Renard, O. Plaidy, Sol. Energy Mater. Sol. Cells 38 (1995) 391.
[27] C. Minero, V. Maurino, E. Pelizzetti, Marine Chem. 58 (1997) 361.
[28] R.W. Matthews, Photocatalysis in water purification: possibilities problems and prospects, in: D.F. Ollis, H. Al-Ekabi (Eds.), Photocatytic Purification and Treatment of Water and Air, Elsevier, Amsterdam, 1993, pp. 121–138.
[29] Y. Mao, C. Schöneich, K.-D. Asmus, Radical mediated degradation mechanisms of helogenated organic compounds as studied by photocatalysis at TiO_2 and by radiation chemistry, in: D.F. Ollis, H. Al-Ekabi (Eds.), Photocatalytic Purification and Treatment of Water and Air, Elsevier, Amsterdam, 1993, pp. 49–65.
[30] K. O'Shea, A. Conde, The reactions of isomeric 2,4-hexadienes on photoexcited TiO_2. Evidence for hole mediated oxidative pathways, in: D.F. Ollis, H. Al-Ekabi (Eds.), Photocatytic Purification and Treatment of Water and Air, Elsevier, Amsterdam, 1993, pp. 707–712.
[31] N. Serpone, D. Lawless, R. Terzian, C. Minero, E. Pelizzetti, Heterogeneous photocatalysis: photochemical conversion of inorganic substances in the environment: hydrogen sulfide, cyanides, and metals, in: E. Pelizzetti, M. Schiavello (Eds.), Photochemical Conversion and Storage of Solar Energy, Kluwer, The Netherlands, 1991, pp. 451–475.
[32] M.R. Prairie, B.M. Stange, L.R. Evans, TiO_2 photocatalytic destruction of organics and the reduction of heavy metals, in: D.F. Ollis, H. Al-Ekabi (Eds.), Photocatytic Purification and Treatment of Water and Air, Elsevier, Amsterdam, 1993, pp. 353–363.
[33] H. Tahiri, N. Serpone, R. Le van Mao, J. Photochem. Photobiol. A: Chem. 93 (1996) 199.
[34] L. Tinucci, E. Borgarello, C. Minero, E. Pelizzetti, Treatment of industrial wastewaters by photocatalytic oxidation in TiO_2, in: D.F. Ollis, H. Al-Ekabi (Eds.), Photocatytic Purification and Treatment of Water and Air, Elsevier, Amsterdam, 1993, pp. 585–594.
[35] R.W. Matthews, J. Catal. 111 (1988) 264.
[36] S. Yamagata, R. Baba, A. Fujishima, Bull. Chem. Soc. Jpn. 62 (1989) 1004.
[37] N. Serpone, A.V. Emeline, Suggested terms and definitions in photocatalysis and radiocatalysis, Int. J. Photoenergy 4 (2002) 91.